

Alkali-Cation-Enhanced Benzylammonium Passivation for Efficient and Stable Perovskite Solar Cells Fabricated Through Sequential Deposition

Jie Cao, ‡^a Junke Jiang, ‡^b Nan Li, ‡^a Yifan Dong,^a Yongheng Jia,^a Shuxia Tao,^{*b} and Ni Zhao^{*a}

^aDepartment of Electronic Engineering, The Chinese University of Hong Kong, Shatin, New Territories, Hong Kong

^bCenter for Computational Energy Research, Department of Applied Physics, Eindhoven University of Technology, P. O. Box 513, 5600 MB, Eindhoven, the Netherlands

‡ These authors contributed equally to this work.

*Correspondence e-mail: nzhao@ee.cuhk.edu.hk; S.X.Tao@tue.nl

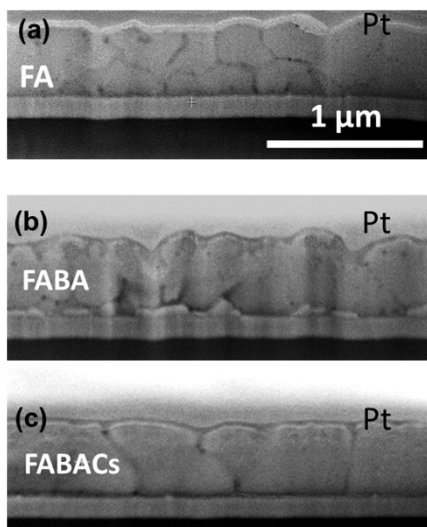


Fig. S1 Cross-sectional SEM images of FA, FABA and FABACs films.

The measured thickness values of the FA, FABA and FABACs samples are 440 nm, 452 nm and 445 nm, respectively. There is a standard deviation of 6 nm in the thickness values. We believe this is a common variation seen in different fabrication batches. Note that we have also measured the thickness of our samples via other means (e.g., stylus profiler) and did not find the FABA samples are systematically thicker than the FA and FABACs samples. A few islanded small grains are observed at the bottom of the FABA perovskite, which might be induced by a special nucleation and crystallization process (Ref. [S1, S2]).

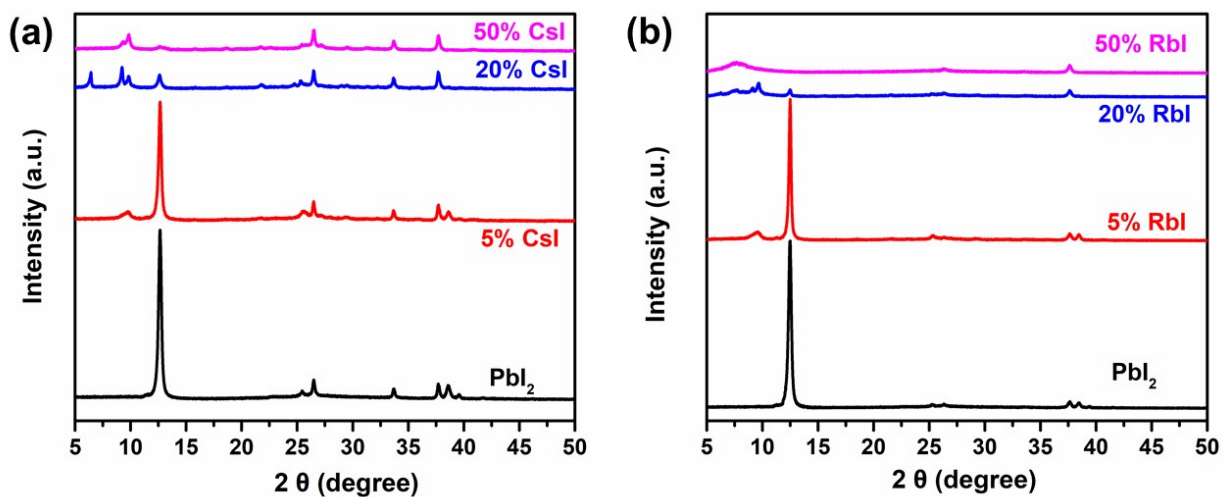


Fig. S2 XRD patterns of the PbI_2 films with and without inclusion of (a) CsI or (b) RbI.

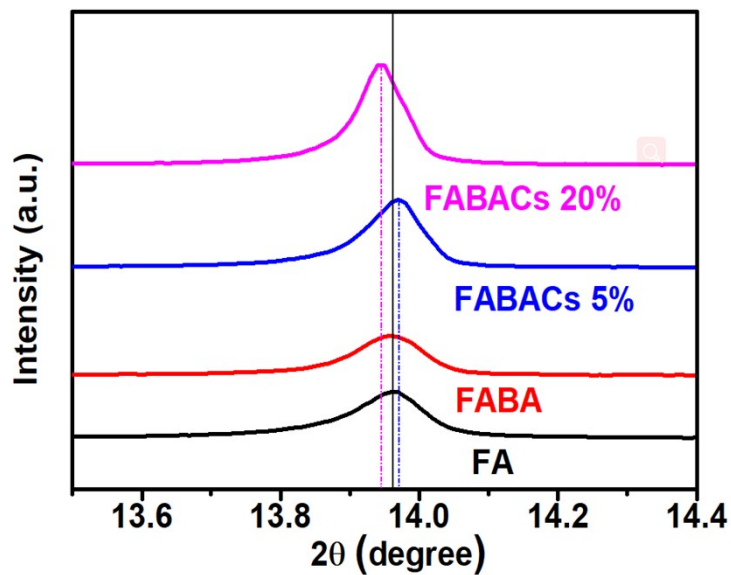


Fig. S3 Perovskite diffraction peaks around 14° extracted from the XRD patterns of FA, FABA and FABACs films.

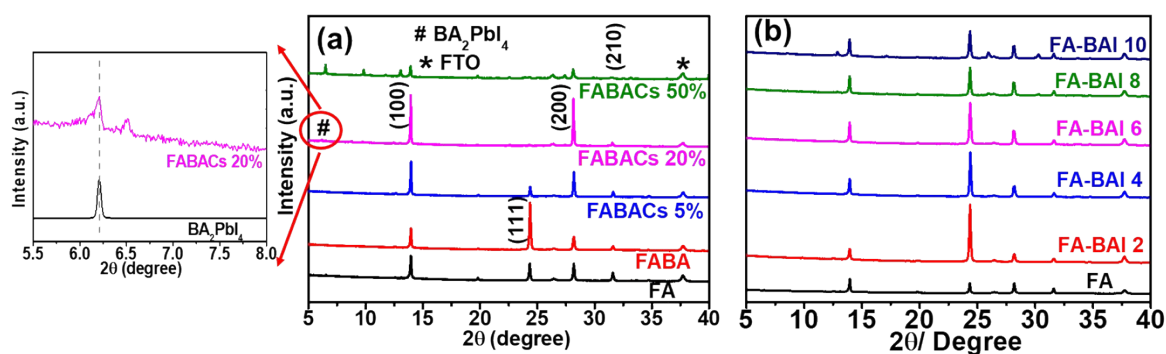


Fig. S4 (a) XRD patterns of FA, FABA and FABACs incorporated with CsI of different molar ratios. (b) XRD patterns of FA and FABA incorporated with BAI of different weight concentration, the number stands for the weight concentration of BAI in the organic mixture solution, unit: mg/mL.

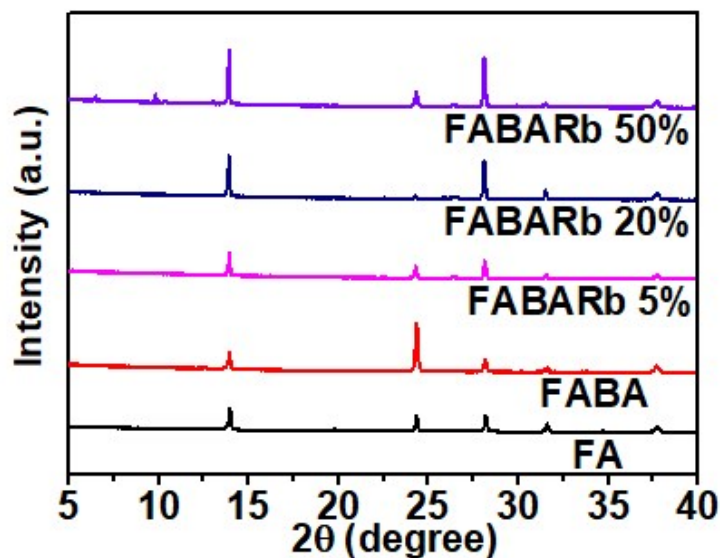


Fig. S5 XRD patterns of FA, FABA and FABARb incorporated with RbI of different molar ratios.

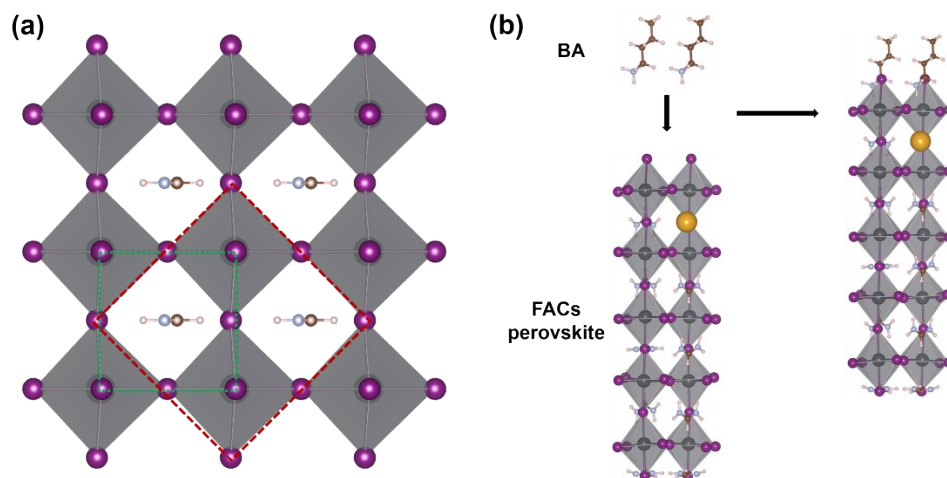


Fig. S6 (a) Scheme of the construction of $\sqrt{2} \times \sqrt{2}$ supercell (top view). The green square indicates the unit cell of cubic FAPbI₃. The red square shows the $\sqrt{2} \times \sqrt{2}$ supercell of cubic FAPbI₃. The BA⁺-passivated model is then constructed by replacing two FA⁺ on the surface with two BA⁺. (b) Schematic representation of the BA⁺-passivated perovskite surfaces (side view).

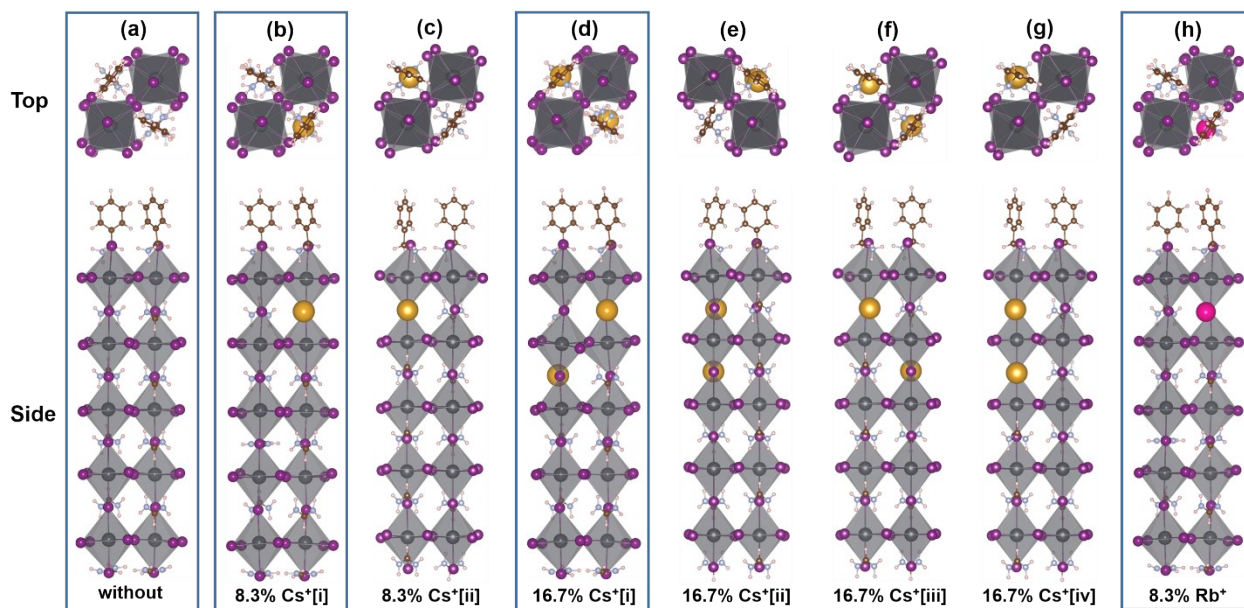


Fig. S7 Top and side views of BA passivated perovskites with (a) 0%, (b) 8.3% Cs⁺[i], (c) 8.3% Cs⁺[ii], (d) 16.7% Cs⁺[i], (e) 16.7% Cs⁺[ii], (f) 16.7% Cs⁺[iii], (g) 16.7% Cs⁺[iv], and (h) 8.3% Rb⁺ in the 3D FAPbI₃ perovskites. For 8.3% Cs⁺, we consider two configurations, and for 16.7% Cs⁺, we consider four configurations. The most stable configurations are highlighted by blue lines. The purple, light blue, brown, light pink, dark grey, dark yellow and rose-red spheres denote I, N, C, H, Pb, Cs and Rb atoms, respectively. The percentage of Cs⁺ and Rb⁺ are calculated as following: when one Cs⁺ substituting for one FA⁺, where twelve A-site cations (ten FA⁺ and two BA⁺) in total, the percentage of Cs⁺ is $1/12 = 8.3\%$.

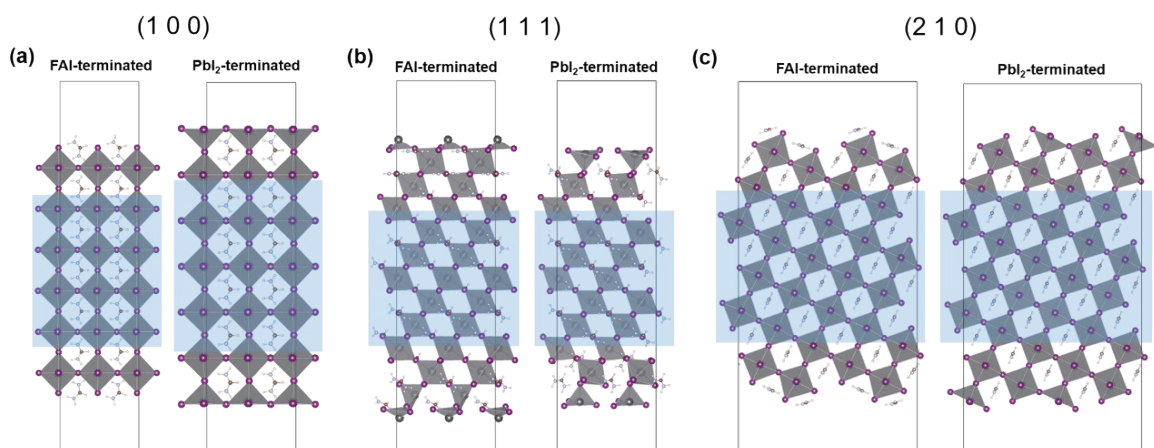


Fig. S8 Structural models of FAPbI₃ surfaces: (1 0 0) (a), (1 1 1) (b) and (2 1 0) (c) with FAI- and PbI₂-terminations, respectively. The layers inside the blue rectangle regions were fixed while the top and bottom layers were relaxed.

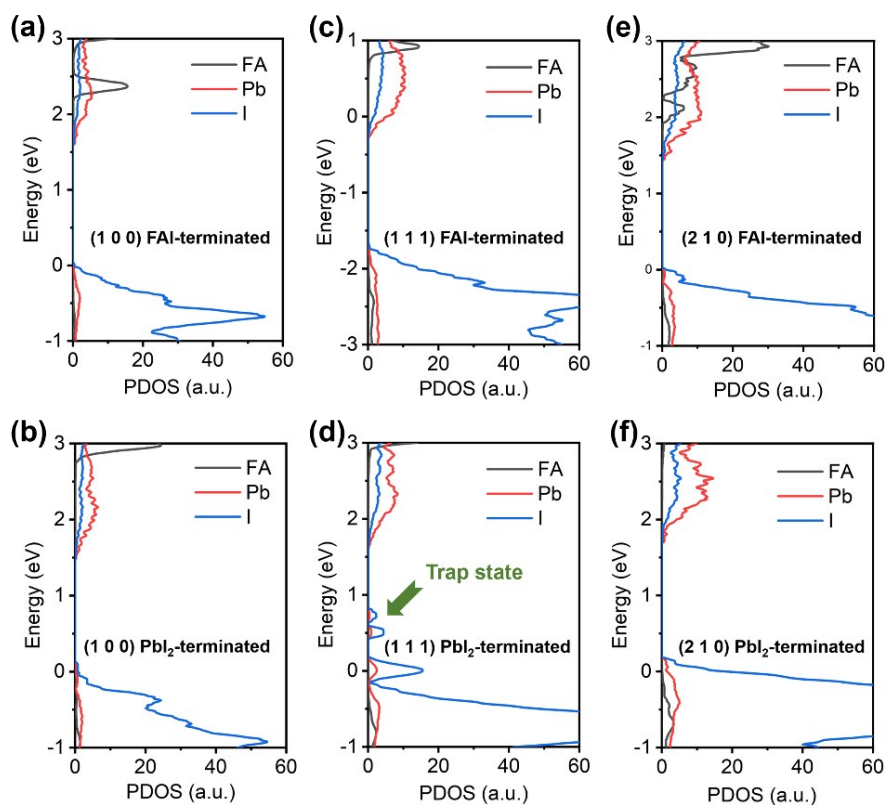


Fig. S9 Projected density of states of FAI- and PbI₂-terminated FAPbI₃ surfaces of (1 0 0) (a, b), (1 1 1) (c, d) and (2 1 0) (e, f).

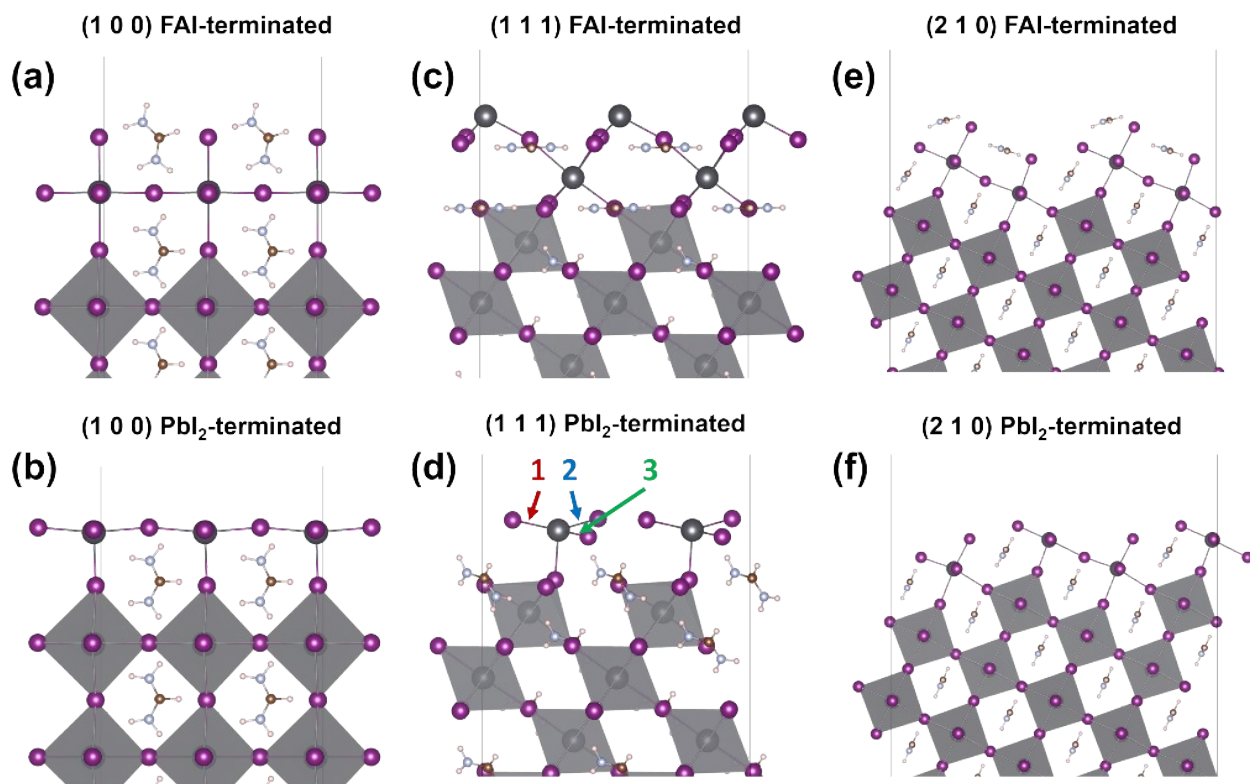


Fig. S10 FAI- and PbI₂-terminated FAPbI₃ surfaces of (1 0 0) (a, b), (1 1 1) (c, d) and (2 1 0) (e, f). The three undercoordinated Pb-I bonds in a unit cell are indicated by red, blue, and green arrow, respectively. The two straight grey lines in the crystal structure indicate the 2×2 slab.

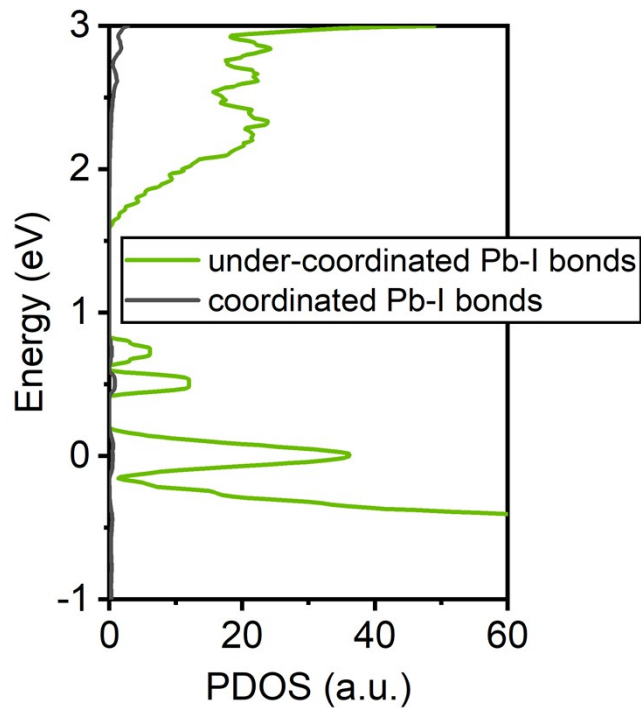


Fig. S11 Projected density of states (PDOSs) of PbI_2 -terminated FAPbI_3 (1 1 1). The green and black lines are the PDOS of atoms from undercoordinated Pb-I bonds on the surface and atoms from other regular Pb-I bonds, respectively.

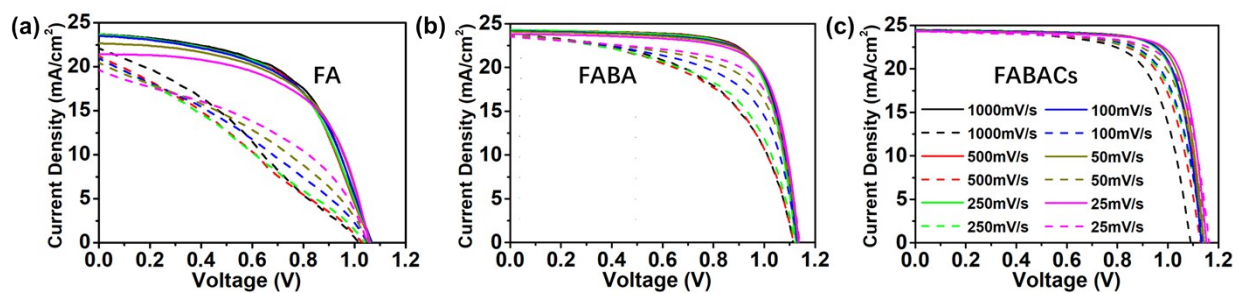


Fig. S12 Reverse scanned (solid lines) and forward scanned (dash lines) J-V curves of (a) FA, (b) FABA and (c) FABACs devices with scan rate from 1000 mV/s to 25 mV/s.

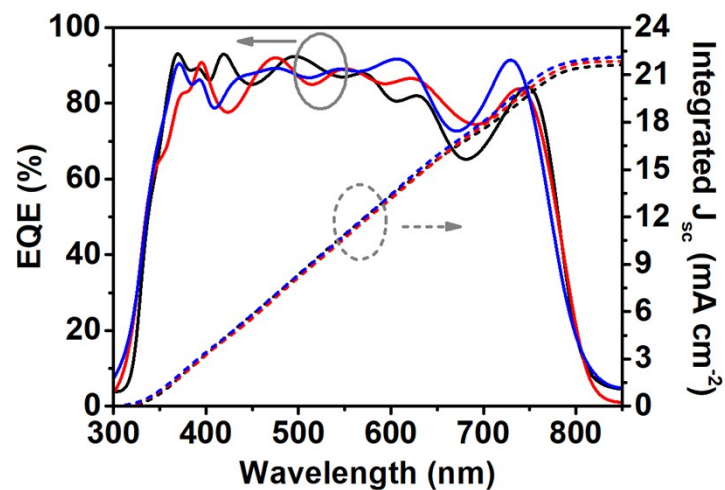


Fig. S13 IPCE spectra (solid line) and integrated current density (dash line) of the corresponding PSCs.

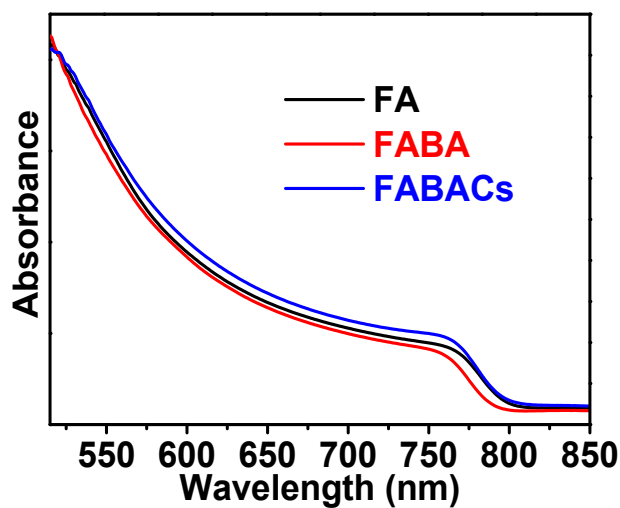


Fig. S14 UV-vis absorption spectra of FA, FABA and FABACs perovskites.

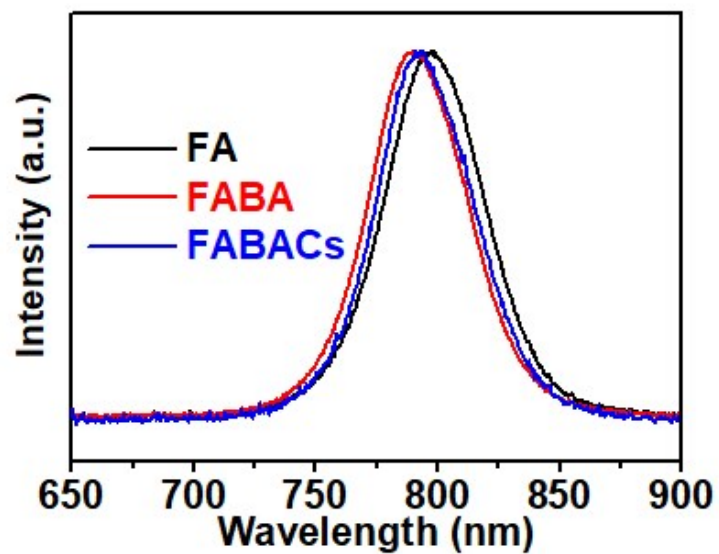


Fig. S15 PL spectra of FA, FABA and FABACs perovskites.

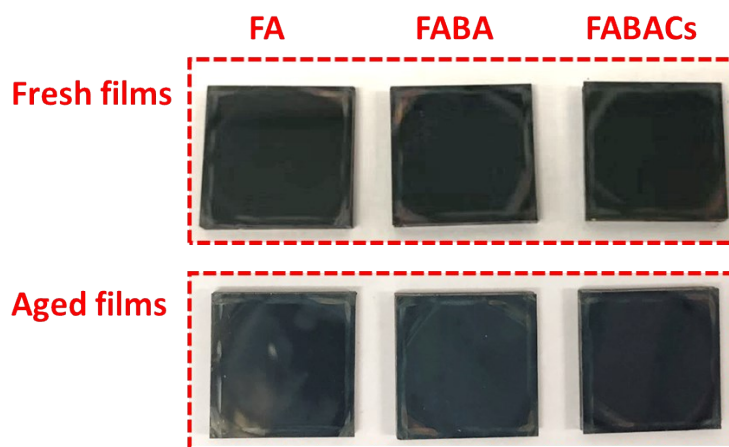


Fig. S16 Photos of the FA, FABA, FABACs samples before (top row) and after (bottom row) aging at 100 °C under two-sun illumination for 8 h.

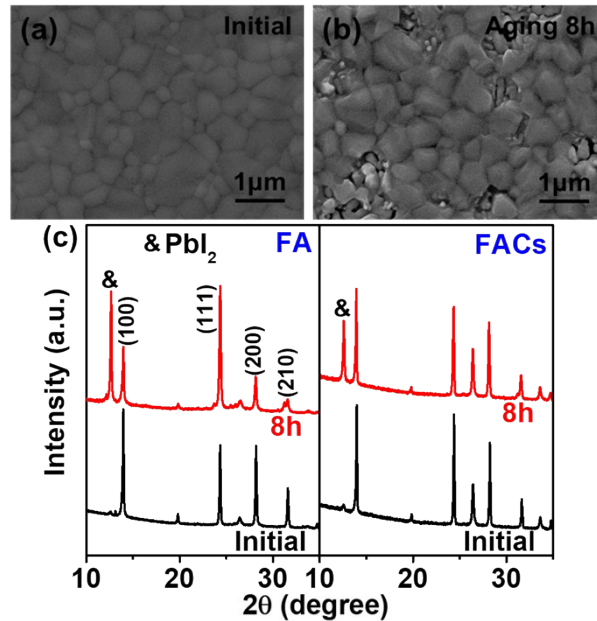


Fig. S17 SEM images of the FACs perovskite: (a) initial film, (b) film after aging at 100 °C for 8 h under a white LED light source with an intensity of 2000 W/m²; (c) XRD patterns of the FA and FACs perovskites after aging at 100 °C for 8 h under a white LED light source with an intensity of 2000 W/m².

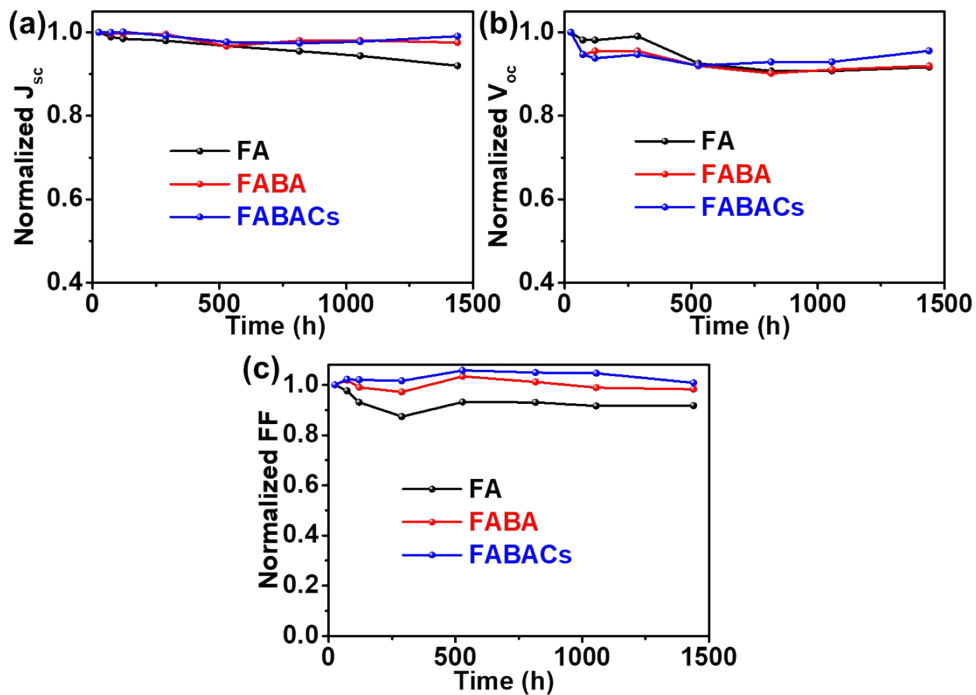


Fig. S18 Variations of (a) J_{sc} , (b) V_{oc} and (c) FF of PSCs based on FA, FABA and FABACs perovskites upon air exposure without encapsulation (humidity level: 60–65%).

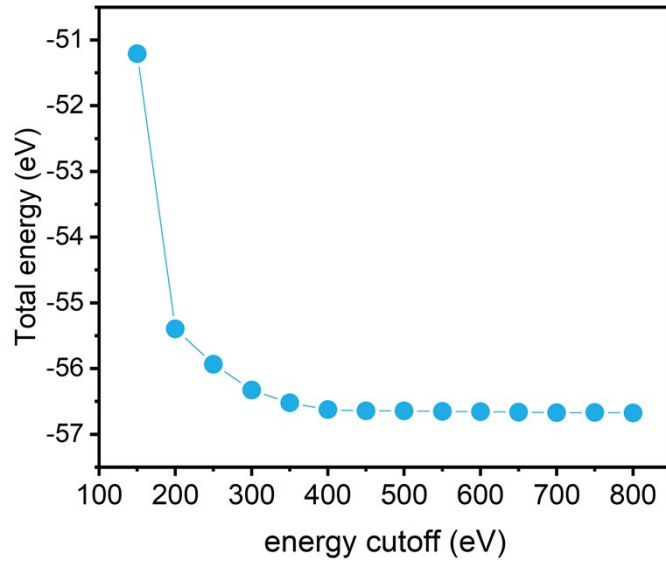


Fig. S19 The total energy convergence with plane-wave energy cutoff for the unit cell of a bulk cubic FAPbI₃.

Table S1. Interface formation energies and structural details of the perovskites: lattice parameters, hydrogen bond lengths (d_1 , d_2 , d_3 and d_4), average bond length d_{av} , and lattice parameter.

Type	Composition	without	8.3% Cs ⁺	16.7% Cs ⁺	8.3% Rb ⁺
Interface formation energy (meV/Å ²)		-317.95	-321.78	-322.35	-323.73
Lattice parameter (Å)	a	9.12	9.08	9.04	9.08
	b	9.18	9.15	9.15	9.10
d_1 (Å)		2.62	2.62	2.60	2.63
d_2 (Å)		2.66	2.68	2.70	2.67
d_3 (Å)		2.64	2.63	2.66	2.60
d_4 (Å)		2.61	2.60	2.60	2.61
d_{av} (Å)		2.63	2.63	2.64	2.63

Table S2. Performance of the photovoltaic devices based on FA and FABA perovskites. The number behind FABA stands for the concentration (mg/mL) of the BAI in the organic mixture solution.

	V_{oc} (V)	J_{sc} (mA·cm ⁻²)	FF (%)	PCE (%)
FA	1.060±0.031	23.409±0.827	66.559±3.320	16.523±1.326
FABA 2	1.124±0.019	23.982±0.924	67.446±5.749	18.148±2.178
FABA 4	1.140±0.014	24.236±0.516	69.324±2.836	19.164±1.129
FABA 6	1.144±0.011	24.139±0.715	67.301±2.962	18.608±1.398
FABA 8	1.082±0.030	24.352±0.427	59.088±3.648	15.586±1.301
FABA 10	0.787±0.130	15.025±1.230	44.494±3.140	5.365±1.029

Table S3. Performance parameters (extracted from reverse scan and forward scan of the J-V curves) of the photovoltaic devices made of FA, FACs, FABA and FABACs perovskites.

		V_{oc} (V)	J_{sc} (mA·cm ⁻²)	FF (%)	PCE (%)
FA	Reverse	1.060±0.031	23.409±0.827	66.559±3.320	16.523±1.326
	Forward	0.978±0.062	23.261±0.261	54.771±9.130	12.448±2.229
FACs	Reverse	1.089±0.017	24.237±0.376	73.925±2.653	19.517±0.870
	Forward	1.021±0.024	24.124±0.371	57.408±3.304	14.146±0.904
FABA	Reverse	1.140±0.014	24.236±0.516	69.324±2.836	19.164±1.129
	Forward	1.112±0.015	24.060±0.894	58.907±2.039	15.768±0.968
FABACs	Reverse	1.145±0.012	24.706±0.433	74.601±2.619	21.132±0.750
	Forward	1.113±0.008	24.451±0.460	68.749±2.444	18.705±0.731

Table S4. Conductivity of the fresh SnO₂ film and the ones coated with FACs and FABACs perovskites and subsequently washed with DMF.

	SnO ₂	SnO ₂ -FACs	SnO ₂ -FABACs
Conductivity (S cm ⁻¹)	1.57×10 ⁻⁴	1.57×10 ⁻⁴	1.55×10 ⁻⁴

References

- 1 C. Liu, Y. Yang, O. A. Syzgantseva, Y. Ding, M. A. Syzgantseva, X. Zhang, A. M. Asiri, S. Dai and M. K. Nazeeruddin, *Adv. Mater.*, 2020, 2002632.
- 2 C. Li, R. Ma, X. He, T. Yang, Z. Zhou, S. Yang, Y. Liang, X. W. Sun, J. Wang, Y. Yan and W. C. H. Choy, *Adv. Energy Mater.*, 2020, **10**, 1903013.